Meng et al. BMC Ophthalmology (2025) 25:121
https://doi.org/10.1186/s12886-025-03948-6

BMC Ophthalmology

RESEARCH

Effects of effective optical zone and decentration on visual quality after smile for different astigmatism types

Xuyun Meng[1], Hui Ding[2], Zhenduo Yang[2], Xiaodan Chen[2], Shisi Hu[2] and Xingwu Zhong[1,2*]

Abstract

Purpose To compare the refractive outcomes and visual quality among different types of astigmatism following SMILE and evaluate effective optical zone (EOZ) features, decentration and their potential effects on visual quality.

Methods This study included 101 left eyes of 101 patients who underwent SMILE. Patients were grouped according to astigmatism types (with-the-rule [WTR], against-the-rule [ATR] and oblique astigmatism) and decentered displacement (major axis > minor axis and major axis < minor axis). We compared the refractive outcomes, visual quality, EOZ and decentration 3 months postoperatively and analyzed correlations between corneal aberrations and EOZ parameters.

Results The visual and refractive outcomes were favorable in different types of astigmatism. The induced corneal aberrations, EOZ and total decentration were comparable among three groups (all $p > .05$). There was a strong positive correlation ($r = .828$, $p < .001$) between preoperative cylinder axis and the angle of EOZ. The postoperative induced changes in spherical aberration (0.02 ± 0.15 vs. 0.08 ± 0.13, $p = .037$), coma (0.22 ± 0.27 vs. 0.36 ± 0.25, $p = .010$), total HOAs (0.28 ± 0.24 vs. 0.42 ± 0.31, $p = .009$) and LOAs (0.16 ± 0.62 vs. 0.49 ± 0.84, $p = .023$) were fewer in group with greater decentered displacement along the major axis than the minor axis.

Conclusions Favorable outcomes were observed in different types of astigmatism. Postoperative refractive errors, visual acuity, and induced corneal aberrations showed no significant differences between groups with WTR, ATR, and oblique astigmatism. The angle of EOZ was closely associated with cylinder axis. EOZ provided greater tolerance to decentration, with fewer induced corneal aberrations along the major axis compared to the minor axis. The combined impacts of EOZ and decentration on visual quality should be noted.

Keywords Small incision lenticule extraction, Effective optical zone, Decentration, Visual quality, Myopic astigmatism

*Correspondence:
Xingwu Zhong
zhongxwu@mail.sysu.edu.cn
[1]State Key Laboratory of Ophthalmology, Zhongshan Ophthalmic Center, Guangdong Provincial Key Laboratory of Ophthalmology and Visual Science, Guangdong Provincial Clinical Research Center for Ocular Diseases, Sun Yat-sen University, Guangzhou 510060, China
[2]Key Laboratory of Ophthalmology, Zhongshan Ophthalmic Center, Hainan Eye Hospital, Sun Yat-sen University, Haikou 570300, China

Introduction

Small incision lenticule extraction (SMILE), a minimally invasive refractive surgery, has been widely adopted for its promising refractive outcomes, rapid nerve recovery, and maintained corneal biomechanics [1–4]. However, SMILE presents challenges in treating astigmatism, with under-correction ranging from 11 to 16% per diopter [5, 6] and visual quality symptoms occurring in about 50–70% of patients with high astigmatism [7]. Therefore, accurate astigmatic correction is crucial to ensuring the efficacy of refractive surgery and patient satisfaction.

Several factors have been identified to impact the effectiveness of SMILE, including refractive correction, cyclotorsion, and optical zone, with the axis of astigmatism being a potential factor as well [8–10]. Oblique astigmatism accounts for 10–18% of all astigmatism cases [11, 12]. Recent studies have reported that oblique astigmatism exhibits more irregular astigmatism than ATR and with-the-rule (WTR) astigmatism [13], which may induce more higher-order aberrations after surgery. Previous studies have shown that WTR astigmatism exhibited more undercorrection than against-the-rule (ATR) or oblique astigmatism [8, 10]. However, the sample size of oblique astigmatism was small in these studies. Additionally, little is known about the visual quality after SMILE for different types of astigmatism.

The effective optical zone (EOZ) is defined as the corneal region that provides quality functional vision after treatment [14]. The area and centration of EOZ are closely related to the postoperative visual quality [15–17]. Notably, the EOZ exhibits an oval shape after myopic astigmatism correction [18, 19]. Given that a larger optical zone treatment may enhance tolerance to decentration, the oval-shaped EOZ may enhance tolerance to decentration along the major axis more than the minor axis. However, to our knowledge, there are no dedicated studies evaluating the EOZ, decentration, and their combined effects on visual quality in patients with different types of astigmatism after SMILE.

Therefore, in the current study, we compared the refractive outcomes and visual quality among different types of astigmatism following SMILE. Additionally, we evaluated EOZ features and decentration using Image J software and analyzed their potential effects on visual quality across different types of astigmatism. Decentration were decomposed into decentered displacement along the major and minor axes, and the visual quality of patients with greater decentered displacement along the major axis was compared to those with greater displacement along the minor axis. These findings have important implications for centration adjustment, programming parameters, and evaluating surgical outcomes for astigmatism correction.

Patients and methods

Ethics approval

This retrospective study was approved by the Ethics Committee of Hainan Eye Hospital at Zhongshan Ophthalmic Center (Sun Yat-sen University, China) (ethics acceptance number: 2023-041-01) and conducted in accordance with the Declaration of Helsinki. Informed consent was obtained from all patients prior to the study.

Patients examinations

This study included 101 left eyes from 101 patients who underwent SMILE surgery at Hainan Eye Hospital between March 2018 and October 2023. The study population comprised 35 eyes with WTR astigmatism (preoperative cylinder axis: 90° ± 30°), 33 eyes with ATR astigmatism (preoperative cylinder axis: 180° to 150° or 0° to 30°), and 33 eyes with oblique astigmatism (preoperative cylinder axis: 31° to 59° or 121° to 149°). The inclusion criteria were preoperative manifest spheres of -0.50D to -10.00D, manifest cylinders of -0.75D to -3.00D, and stable refraction for more than 1 year. Patients with a history of other ocular conditions, such as keratoconus, cataract, uveitis, ocular trauma or surgery, and systemic diseases were excluded.

All patients underwent the following clinical examinations preoperatively and 3 months postoperatively: slit-lamp examination, fundus examination, uncorrected distance visual acuity (UDVA), corrected distance visual acuity (CDVA), manifest refraction, pupil size (keratogragh 5 M, OCULUS Optikgeräte GmbH, Wetzlar, Germany), corneal tomography (Pentacam AXL, OCULUS Optikgeräte GmbH, Wetzlar, Germany), and corneal aberrations (Pentacam AXL, OCULUS Optikgeräte GmbH, Wetzlar, Germany).

Surgical technique

All SMILE standard procedures were performed using the VisuMax femtosecond laser (Carl Zeiss Meditec AG, Jena, Germany) with parameters as follows: pulse energy of 135–140 nJ; cap thickness of 120 μm; cap diameter of 7.5 mm; programed optical zone of 6.5 mm and a transition zone of 0.1 mm for astigmatism; incision width of 2 mm; incision position at 140°. The details surgical procedure has been described by Taneri et al. [20]. All surgical procedures were performed by the same surgeon (XZ). A single nomogram was used for all types of astigmatism.

EOZ area and decentration measurements

EOZ was measured based on the difference map of the tangential curvature between preoperative and 3 months postoperative measurements in Pentacam. ImageJ software (V 2.1.0) was used to automatically recognize the boundary and calculate the area of the EOZ, where the

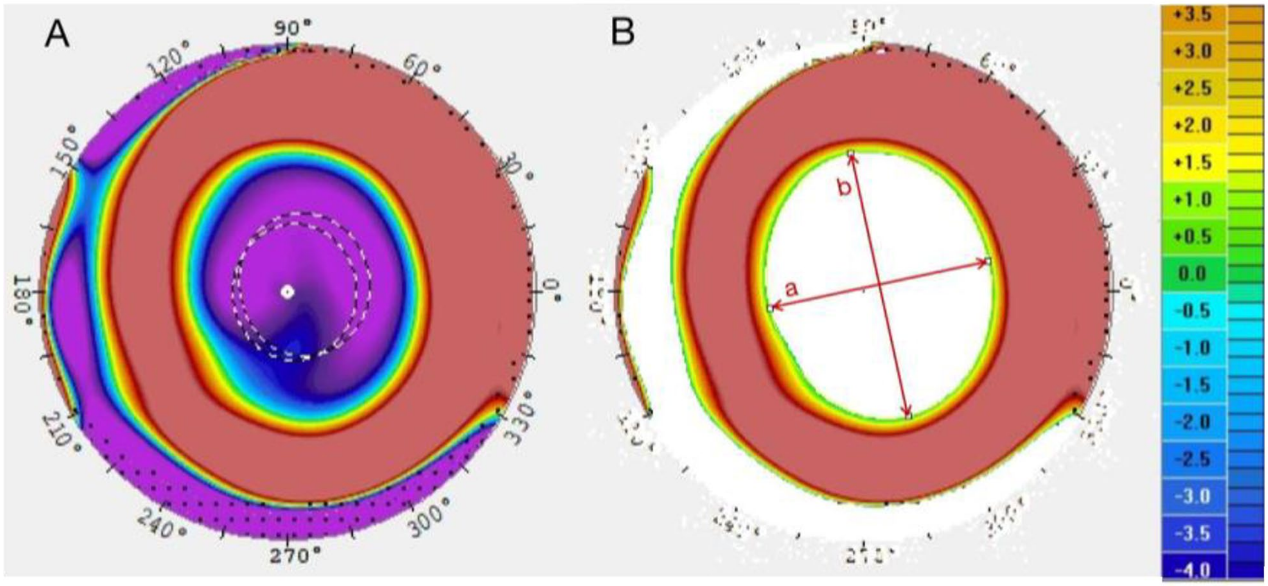

Fig. 1 Illustration of postoperative effective optical zone (EOZ) measurements. (**A**) Original tangential corneal curvature difference map. (**B**) EOZ area, major axis (**a**), and minor axis (**b**) measured using ImageJ software

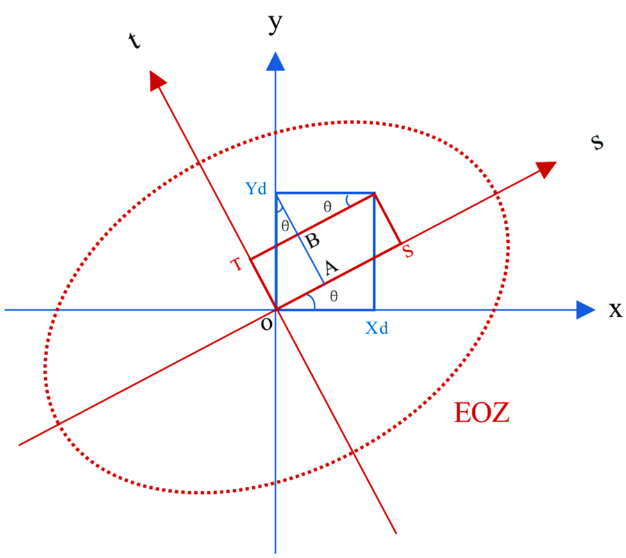

Fig. 2 Measuring decentered displacements along the major (s) and minor (t) axes. The decentered displacement along the major axis was S and along the minor axis was T

tangential curvature difference was zero and shown in green [21]. The difference map was adjusted using "Color Threshold," the area was measured, and the Fit Ellipse function was used to determine the center (X, Y), angle (θ), and the major and minor axes of the best-fitted ellipse of the EOZ (Fig. 1A and B). To facilitate correlation analysis between EOZ angle and cylinder axis, adjustments were made to ensure consistent ranges. 180° was added to the EOZ angle when it ranged from 0° to 45° and the cylinder axis ranged from 135° to 180°. Similarly, 180° was added to the cylinder axis when the EOZ angle ranged from 135° to 180° and the cylinder axis ranged from 0° to 45°.

The corneal vertex coordinates were measured as (X_1, Y_1). The horizontal decentered displacement was $X_d = (X - X_1)$, and the vertical decentered displacement was $Y_d = (Y_1 - Y)$. The total decentered displacement was $\sqrt{(X - X_1)^2 + (Y_1 - Y)^2}$. For convenience, the coordinate system was established based on the best-fitted ellipse, with the ellipse's center as the origin and the major and minor axes as the s and t axes, respectively. The corneal vertex coordinates (S, T) were calculated as follows: $S = OA + AS = Y_d\sin(\theta) + X_d\cos(\theta)$, $T = AY_d - BY_d = Y_d\cos(\theta) - X_d\sin(\theta)$ (Fig. 2). The decentered displacement along the major axis was S and along the minor axis was T.

Statistical analysis

All data were analyzed by SPSS (version 26.0; SPSS, Inc.). Data normality was defined by the Kolmogorov-Smirnov test. One-way ANOVA test, Kruskal–Wallis test, Wilcoxon signed rank test, and independent-sample t-test were used for statistical analysis. Pearson correlation was used to detect the correlations of induced corneal aberrations and EOZ area, major axis, and minor axis. Statistically significant was defined as a P value < 0.05. A sample size of 28 achieves 90% power to detect a difference of 0.05 between the null hypothesis mean of 0.00 and the alternative hypothesis mean of 0.05 using a two-sided hypothesis test with a significance level of 0.0167 (0.05/3) for multiple testing. Sample size was calculated by software PASS 16 (NCSS, LLC, USA).

Results

General data

This study included 101 eyes of 101 patients: 35 eyes in the WTR astigmatism group, 33 eyes in the ATR astigmatism group, and 33 eyes in the oblique astigmatism group. The cohort comprised 38 men and 63 women, with a mean age of 26.95 years (range: 18 to 47 years). There were no significant differences in correction, preoperative visual acuity, pupil size, preoperative pupillary offset, programmed optical zone, ablation depth, and ablation ratio among the three groups (Table 1). No complications were observed during or after the surgery.

Efficacy, safety and predictability

The refractive outcomes of 101 eyes after SMILE are shown in Fig. 3. At 3 months, 96 (95.1%) eyes achieved a UDVA of 20/20, and 97 (96.0%) eyes maintained or gained one or more lines of CDVA compared to preoperative UDVA (Fig. 3A and B). Only two eyes lost one line of CDVA compared to the preoperative value (Fig. 3C). Predictability is shown in Fig. 3D and E. All eyes were within ±1.00 D and 97.0% of eyes were within ±0.50 D of the attempted postoperative SE (Fig. 3E). The cylinder predictability was 82.2% (83 eyes) within ±0.25 D, 98.0% (99 eyes) within ±0.50 D, and 100% (101 eyes) within ±1.00 D of the attempted postoperative cylinder (Fig. 3G). The mean SIA was slightly undercorrected compared to the mean TIA (Fig. 3H).

Three months after the surgery, the efficacy indexes (postoperative UDVA/preoperative CDVA) were 1.10±0.11, 1.12±0.11, and 1.11±0.12, and the safety indexes (postoperative CDVA/ preoperative CDVA) were 1.13±0.10, 1.17±0.11, and 1.13±0.11 in the WTR, ATR and oblique astigmatism groups, respectively. There were no statistically significant differences in mean efficacy index (P=.727) or safety index (P=.205) among the three groups.

Refractive errors, visual outcomes, and induced corneal aberrations

Postoperative refractive errors, visual acuity, and induced corneal wavefront aberrations were shown in Table 2. There were no significant differences in postoperative refractive errors, visual acuity, spherical aberration, coma, trefoil, total HOAs, and LOAs changes among groups of different astigmatism types (Table 2).

EOZ and decentration

The postoperative EOZ area, the major axis, and the minor axis showed no significant difference among WTR, ATR and oblique astigmatism groups (Table 3). The angle of the fit ellipse of EOZ was positively correlated with the axis of preoperative astigmatism (r=.828, p<.001) (Figs. 4 and 5).

As summarized in Table 3, there was no significant difference in the total decentration, horizontal displacement, vertical displacement, displacement along major

Table 1 Preoperative and surgical parameters of patients in different astigmatism types

Parameter	WTR	ATR	Oblique	*P* value
Preoperative characteristic Patients' eyes, n	35, 35	33, 33	33, 33	
Age, y	24.43±7.16	29.03±6.06	27.55±5.87	
Sex, % women	57.1%	54.5%	75.7%	
Sphere, D	-5.13±1.83 (-8.75, -1.75)	-4.53±1.54 (-7.50, -1.00)	-4.70±1.63 (-8.00, -2.00)	0.317‡
Cylinder, D	-1.17±0.34 (-1.75, -0.75)	-1.07±0.44 (-2.75, -0.75)	-1.04±0.41 (-2.50, -0.75)	0.078†
Spherical equivalent, D	-5.71±1.83 (-9.25, -2.50)	-5.06±1.52 (-7.88, -1.63)	-5.22±1.65 (-8.50, -2.38)	0.249‡
UDVA (logMAR)	1.25±0.21 (0.60, 1.70)	1.28±0.23 (0.70, 1.70)	1.30±0.27 (0.70, 2.00)	0.490†
CDVA (logMAR)	0.00±0.00 (0.00, 0.00)	0.01±0.03 (0.00, 0.10)	0.00±0.01 (0.00, 0.05)	0.212†
Scotopic pupil size	6.43±0.73 (5.10, 8.10)	6.31±0.62 (4.90, 7.30)	6.27±0.77 (4.40, 7.90)	0.780†
Mesopic pupil size	5.89±0.76 (4.70, 7.60)	5.82±0.66 (3.80, 6.80)	5.76±0.76 (4.00, 7.50)	0.761‡
Photopic pupil size	4.03±0.71 (2.90, 5.50)	4.04±0.66 (2.70, 5.60)	3.90±0.73 (2.70, 5.40)	0.649‡
Preoperative pupillary offset, mm	0.19±0.10 (0.05, 0.49)	0.15±0.10 (0.00, 0.43)	0.16±0.07 (0.04, 0.36)	0.213‡
|Preoperative pupillary offset (x-axis)|, mm	0.10±0.06 (0.00, 0.23)	0.08±0.09 (0.00, 0.36)	0.11±0.07 (0.00, 0.33)	0.090†
|Preoperative pupillary offset (y-axis)|, mm	0.14±0.10 (0.00, 0.49)	0.11±0.08 (0.00, 0.41)	0.09±0.07 (0.01, 0.24)	0.154†
Surgical Parameter				
Programmed optical zone, mm	6.5	6.5	6.5	
Ablation depth, mm	108.54±28.14 (56.00, 164.00)	100.30±22.27 (52.00, 142.00)	103.52±24.26 (60.00, 149.00)	0.396‡
Ablation ratio (ablation depth/ CCT)	0.20±0.05 (0.10, 0.32)	0.19±0.04 (0.10, 0.28)	0.19±0.04 (0.11, 0.27)	0.519‡

D, diopter; UDVA, uncorrected distance visual acuity; CDVA, corrected distance visual acuity; CCT, center corneal thickness

†Kruskal–Wallis test

‡One-way Anova test

§Values are presented as mean±standard deviation (range)

*P values less than 0.05 indicating statistical significance are marked in bold

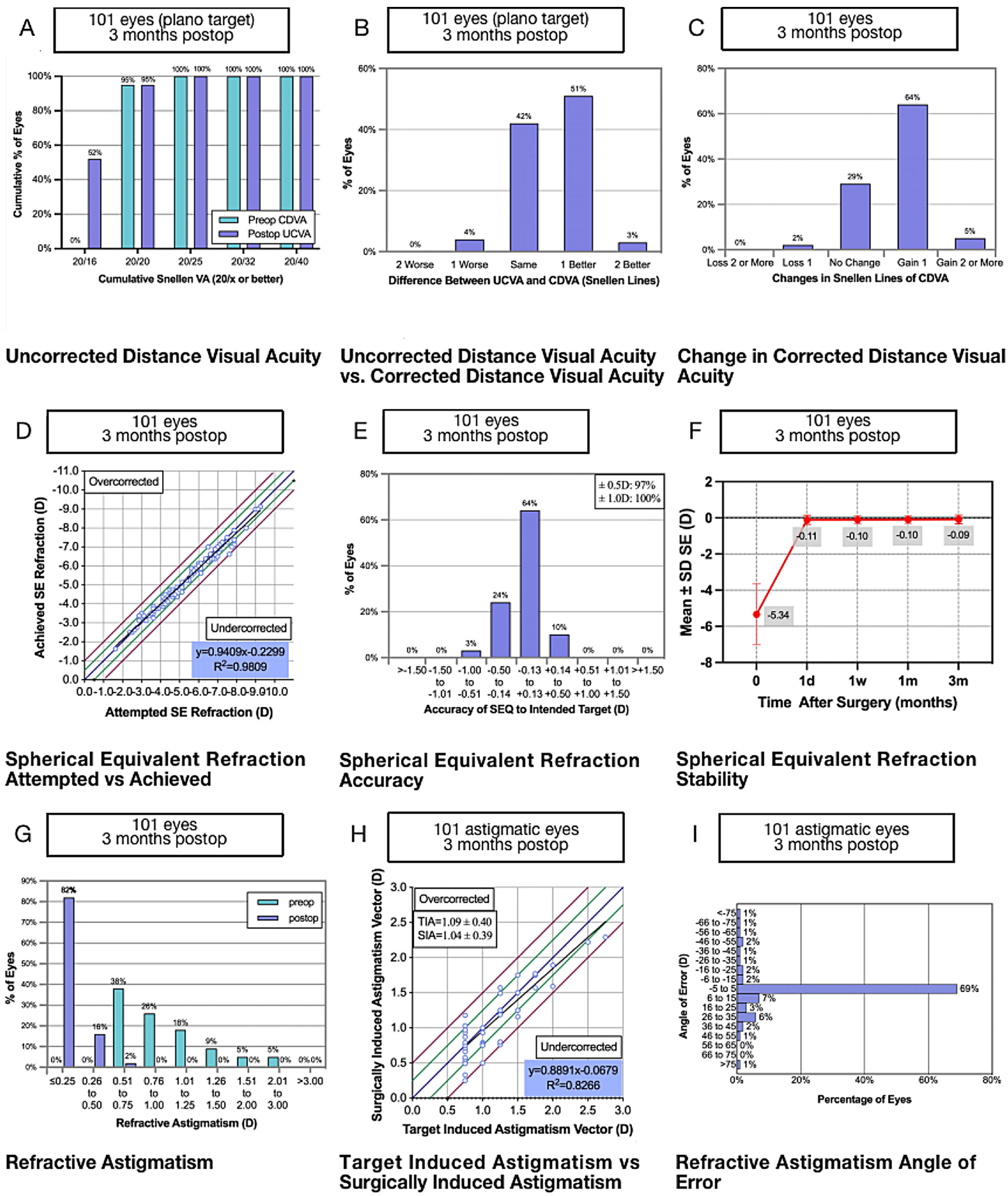

Fig. 3 Visual and refractive outcomes of 101 eyes after small incision lenticule extraction. (**A**) Cumulative 3-month postoperative uncorrected distance visual acuity (UDVA) and preoperative corrected distance visual acuity (CDVA). (**B**) Difference of postoperative UDVA vs. preoperative CDVA in the Snellen lines. (**C**) Changes in Snellen lines of CDVA postoperatively. (**D**) Attempted vs. achieved changes in spherical equivalent refraction (SE) at 3 months post-surgery. (**E**) Accuracy of SE to the intended target. (**F**) SEQ stability. (**G**) Distribution of cylinders preoperative and 3 months postoperatively. (**H**) Surgically induced astigmatism vs. target induced astigmatism. (**I**) Distribution of refractive astigmatism angle of error at 3 months postoperatively. D = diopters; SIA = surgically induced astigmatism; TIA = target induced astigmatism

Table 2 Comparison of refractive errors, visual outcomes, and induced corneal aberrations

Parameter	WTR	ATR	Oblique	P value
Postoperative sphere (D)	-0.01 ± 0.23 (-0.75, 0.50)	0.02 ± 0.22 (-0.50, 0.50)	-0.03 ± 0.25 (-0.75, 0.50)	0.810†
Postoperative cylinder (D)	-0.14 ± 0.20 (-0.50, 0.00)	-0.20 ± 0.22 (-0.75, 0.00)	-0.11 ± 0.20 (-0.75, 0.00)	0.141†
Postoperative SE (D)	-0.10 ± 0.25 (-1.00, 0.50)	-0.08 ± 0.23 (-0.50, 0.50)	-0.09 ± 0.25 (-0.75, 0.50)	0.953†
UDVA (logMAR)	-0.04 ± 0.05 (-0.08, 0.10)	-0.04 ± 0.04 (-0.08, 0.00)	-0.04 ± 0.05 (-0.08, 0.05)	0.973†
CDVA (logMAR)	-0.05 ± 0.04 (-0.08, 0.05)	-0.06 ± 0.03 (-0.08, 0.00)	-0.05 ± 0.04 (-0.08, 0.05)	0.324†
Spherical aberration (μm)	0.08 ± 0.15 (-0.20, 0.42)	0.04 ± 0.13 (-0.28, 0.37)	0.02 ± 0.15 (-0.33, 0.34)	0.205‡
Coma (μm)	0.30 ± 0.29 (-0.50, 0.96)	0.30 ± 0.24 (-0.01, 1.25)	0.26 ± 0.27 (-0.65, 0.82)	0.838‡
Trefoil (μm)	0.00 ± 0.07 (-0.24, 0.20)	0.04 ± 0.11 (-0.13, 0.41)	0.03 ± 0.08 (-0.11, 0.23)	0.192‡
Total HOAs (μm)	0.37 ± 0.32 (-0.34, 1.28)	0.34 ± 0.27 (-0.10, 1.28)	0.31 ± 0.25 (-0.38, 0.81)	0.655‡
LOAs (μm)	0.18 ± 0.77 (-0.91, 2.36)	0.53 ± 0.76 (-1.52, 1.80)	0.25 ± 0.68 (-1.15, 1.68)	0.068†

SE, spherical equivalent; D, diopter; UDVA, uncorrected distance visual acuity; CDVA, corrected distance visual acuity

†Kruskal–Wallis test

‡One-way Anova test

§Values are presented as mean ± standard deviation (range)

*P values less than 0.05 indicating statistical significance are marked in bold

Table 3 EOZ area, major axis, minor axis, and decentration in subgroup analysis

Parameter	WTR	ATR	Oblique	P value
Area, mm^2	23.87 ± 3.37 (18.29, 33.91)	24.97 ± 3.03 (18.07, 33.97)	24.67 ± 3.17 (21.04, 33.73)	0.179†
Major axis, mm	5.80 ± 0.45 (4.92, 7.11)	6.02 ± 0.49 (4.82, 7.05)	5.86 ± 0.42 (5.28, 6.90)	0.126†
Minor axis, mm	5.22 ± 0.38 (4.66, 6.32)	5.27 ± 0.28 (4.67, 6.14)	5.35 ± 0.33 (5.05, 6.40)	0.336†
Decentered displacement (mm)				
Total	0.35 ± 0.14 (0.12, 0.69)	0.39 ± 0.17 (0.07, 0.70)	0.39 ± 0.16 (0.04, 0.67)	0.498‡
Horizontal	0.23 ± 0.14 (0.01, 0.66)	0.24 ± 0.16 (0.03, 0.58)	0.28 ± 0.17 (0.02, 0.63)	0.413†
Vertical	0.23 ± 0.13 (0.00, 0.52)	0.26 ± 0.17 (0.03, 0.70)	0.22 ± 0.14 (0.01, 0.53)	0.544‡
Along major axis	0.22 ± 0.12 (0.01, 0.47)	0.24 ± 0.17 (0.02, 0.69)	0.25 ± 0.17 (0.00, 0.55)	0.818†
Along minor axis	0.23 ± 0.16 (0.03, 0.55)	0.25 ± 0.18 (0.01, 0.62)	0.23 ± 0.17 (0.02, 0.60)	0.881†

†Kruskal–Wallis test

‡One-way Anova test

§Values are presented as mean ± standard deviation (range)

*P values less than 0.05 indicating statistical significance are marked in bold

axis and minor axis among WTR, ATR and oblique astigmatism groups.

We speculated that the oval shaped EOZ may enhance more tolerance to decentration along the major axis than along the minor axis. Therefore, the traditional horizontal and vertical decentered displacements were transformed into displacements along the major and minor axes of the EOZ (Figs. 2 and 6). For further analysis, patients were divided into two groups: group A (major axis displacement > minor axis displacement) and group B (major axis displacement < minor axis displacement). The outcomes of these groups were compared.

There were no significant differences in preoperative refractive errors, decentration, decentered displacement differences between the major and minor axes, pupil size, pupillary offset, ablation depth and ablation ratio between group A and group B. As shown in Table 4, there were no significant difference in UDVA, CDVA, postoperative sphere, cylinder, and SE between the two groups. However, the significant differences were observed in induced spherical aberration, coma, total HOAs, and LOAs between two groups ($P = .037$, $P = .010$, $P = .009$, and $P = .023$, respectively).

Correlation analyses

The relationship between induced corneal aberrations and EOZ area, major axis, and minor axis in different astigmatism types was summarized in Table 5. Correlation tests revealed that increases in spherical aberration correlated with EOZ area, major axis, and minor axis in the WTR, ATR, and oblique astigmatism groups. Additionally, in the WTR and ATR astigmatism groups, increases in coma and total HOAs correlated with EOZ area, major axis, and minor axis. In the ATR group, increases in LOAs correlated with EOZ area and major axis.

The correlations between induced corneal aberrations and total decentration, horizontal and vertical displacement, and displacement along the major and minor axes was summarized in Table 6. Increased total decentration and vertical displacement correlated positively with coma and total HOAs. Increased horizontal displacement correlated positively with spherical aberration and total HOAs. Displacement along the major axis showed a negative correlation with LOAs, while displacement along the minor axis correlated positively with spherical aberration, coma, total HOAs, and LOAs. No statistically significant correlation was observed between preoperative astigmatism and any decentration component.

Discussion

This study demonstrates that SMILE surgery yielded favorable visual and refractive outcomes in myopic astigmatism, exhibiting good efficacy, safety, and

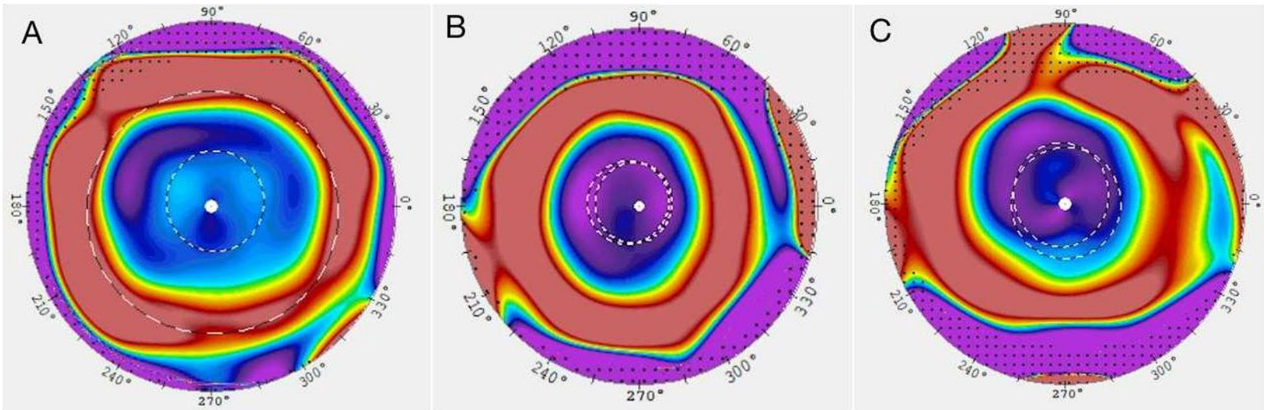

Fig. 4 The effective optical zone (EOZ) in different astigmatism types on tangential curvature difference map. The EOZ margin, where the tangential curvature difference was zero, was shown in green. (**A**) The EOZ of with-the-rule astigmatism was horizontally elliptical. (**B**) The EOZ of against-the-rule astigmatism was vertically elliptical. (**C**) The EOZ of oblique astigmatism was obliquely elliptical

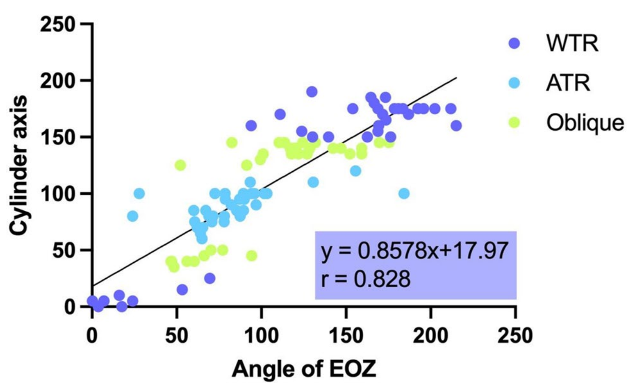

Fig. 5 The correlation between the angle of effective optical zone (EOZ) and cylinder axes

predictability. No significant differences were observed in postoperative refractive errors, visual acuity, or induced corneal aberrations between groups with WTR, ATR, and oblique astigmatism. These findings align with a previous study [10] suggesting that astigmatism correction with SMILE is predictable across different astigmatism types. Additionally, for astigmatism ≥ 0.5D, the resultant astigmatism was not associated with its preoperative classification. This study is the first to compare postoperative induced corneal aberrations across different astigmatism types. While previous studies have suggested that oblique astigmatism is associated with more irregular astigmatism, including asymmetry and higher-order irregularities [13], our study did not find significant differences in induced HOAs between the three groups.

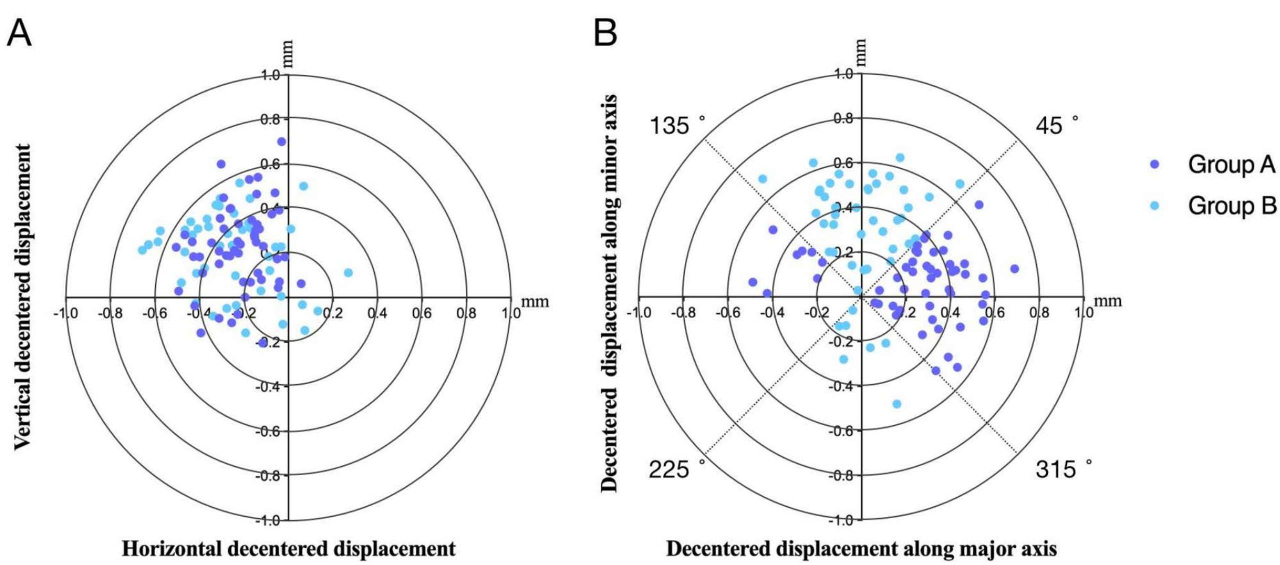

Fig. 6 Scatterplot showing the distribution of decentered displacement. (**A**) Traditional horizontal and vertical decentered displacements. (**B**) Decentered displacements along the major and minor axes

Table 4 Comparison of visual and refractive outcomes and induced corneal aberrations according to decentered displacement along major and minor axes

	Group A (n = 54)	Group B (n = 47)	P value
UDVA (logMAR)	-0.04 ± 0.04 (-0.08, 0.05)	-0.04 ± 0.05 (-0.08, 0.10)	0.844†
CDVA (logMAR)	-0.05 ± 0.04 (-0.08, 0.05)	-0.06 ± 0.04 (-0.08, 0.00)	0.763†
Postoperative sphere (D)	0.02 ± 0.21 (-0.50, 0.50)	-0.04 ± 0.25 (-0.75, 0.50)	0.230†
Postoperative cylinder (D)	-0.12 ± 0.19 (-0.75, 0.00)	-0.18 ± 0.22 (-0.75, 0.00)	0.190†
Postoperative SE (D)	-0.05 ± 0.21 (-0.50, 0.50)	-0.13 ± 0.28 (-1.00, 0.50)	0.287†
Spherical aberration (μm)	0.02 ± 0.15 (-0.33, 0.38)	0.08 ± 0.13 (-0.12, 0.42)	0.037‡
Coma (μm)	0.22 ± 0.27 (-0.65, 0.96)	0.36 ± 0.25 (-0.01, 1.25)	0.010‡
Trefoil (μm)	0.01 ± 0.09 (-0.24, 0.25)	0.05 ± 0.09 (-0.10, 0.41)	0.070†
Total HOAs (μm)	0.28 ± 0.24 (-0.34, 0.92)	0.42 ± 0.31 (-0.38, 1.28)	0.009‡
LOAs (μm)	0.16 ± 0.62 (-1.15, 1.47)	0.49 ± 0.84 (-1.52, 2.36)	0.023‡

UDVA, uncorrected distance visual acuity; CDVA, corrected distance visual acuity; D, diopter; SE, spherical equivalent; HOAs, higher-order aberrations; LOAs, lower-order aberrations

†Wilcoxon Signed Rank Test

‡Independent-Sample t-test

§Values are presented as mean ± standard deviation (range)

*P values less than 0.05 indicating statistical significance are marked in bold

Moreover, we focused on the EOZ after SMILE for different types of astigmatism correction. EOZ was defined as the area of the corneal surface that provides quality functional vision after laser sculpting [14]. Several methods for assessing EOZ have been proposed, including region growing algorithms, ray-tracing approach, and corneal topography [22–24]. While these methods have their strengths, they are often computationally complex, limiting their widespread adoption, or they require manual measurements that are both imprecise and time-consuming. In this study, we utilized the tangential curvature difference map from Scheimpflug tomography to determine the EOZ, based on previous studies [18, 21]. The margin of the EOZ was defined as the change in the zero-diopter line on the subtractive map. Tangential curvature analysis is highly sensitive to localized alterations in the curvature of the anterior corneal surface. The repeatability of EOZ measurement using this approach has been demonstrated by Hou et al. [21]. We further enhanced this by using ImageJ software to automatically delineate the EOZ boundary on the tangential curvature difference map, resulting in both accurate and efficient measurements, and eliminating the subjectivity of manual assessment. For oval shaped EOZ in myopic astigmatism, the Fit Ellipse function in ImageJ provided multidimensional parameters for EOZ evaluation, including area, major axis, minor axis, and angle. The area, major axis, and minor axis showed no significant differences among different types of astigmatism. However, the angle of the EOZ major axis was closely associated with the preoperative cylinder axis, indicating that the EOZ diameter was larger on the flat axis than on the steep axis, regardless of the cylinder axis orientation. Similarly, previous studies have reported the EOZ was oval shaped after SMILE in myopic astigmatism [18, 19]. Wang et al. [16] reported that the corneal curvature change of steep keratometry was greater than that of flat keratometry in moderate and high astigmatism, indicating a smaller corneal curvature change on the axis of the cylinder. According to the Munnerlyn's formula, $t = \frac{S^2 D}{3}$, we speculated that when the refractive correction of cornea (D) on the flat axis is smaller than on the steep axis and the sculpting depth t is constant, the optical area S increases, resulting in a larger EOZ diameter on the flat axis.

Larger optical zone treatment may increase the tolerance of decentration [25]. Therefore, we speculated that

Table 5 Correlation between induced corneal aberrations and EOZarea, major axis, and minor axis in different astigmatism types

Induced corneal aberration (μm)	WTR			ATR			Oblique		
	Area, mm^2	Major axis, mm	Minor axis, mm	Area, mm^2	Major axis, mm	Minor axis, mm	Area, mm^2	Major axis, mm	Minor axis, mm
Spherical aberration	-0.735 (< 0.001)*	-0.722 (< 0.001)*	-0.648 (< 0.001)*	-0.667 (< 0.001)*	-0.589 (< 0.001)*	-0.602 (< 0.001)*	-0.508 (0.003)*	-0.427 (0.013)*	-0.522 (0.002)*
Coma	-0.409 (0.015)*	-0.404 (0.016)*	-0.354 (0.037)*	-0.501 (0.003)*	-0.464 (0.006)*	-0.460 (0.007)*	-0.302 (0.088)	-0.249 (0.162)	-0.324 (0.066)
Trefoil	0.048 (0.785)	0.206 (0.235)	-0.126 (0.472)	-0.008 (0.964)	-0.075 (0.677)	0.099 (0.585)	0.209 (0.242)	0.260 (0.144)	0.115 (0.523)
Total HOAs	-0.612 (< 0.001)*	-0.577 (< 0.001)*	-0.574 (< 0.001)*	-0.505 (0.003)*	-0.492 (0.004)*	-0.417 (0.016)*	-0.333 (0.058)	-0.298 (0.092)	-0.322 (0.068)
LOAs	-0.223 (0.197)	-0.221 (0.202)	-0.202 (0.244)	-0.380 (0.029)*	-0.418 (0.015)*	-0.234 (0.190)	-0.186 (0.300)	-0.206 (0.250)	-0.142 (0.430)

EOZ, effective optical zone; WTR, with-the-rule astigmatism; ATR, against-the-rule astigmatism; HOAs, higher-order aberrations; LOAs, lower-order aberrations

*P value less than 0.05 showing statistical significance

Table 6 Correlation between induced corneal aberrations and total decentration, horizontal and vertical displacement, and displacement along the major and minor axes

Induced corneal aberration (μm)	Decentration				
	Total	Horizontal Displacement	Vertical Displacement	Displacement Along the Major Axis	Displacement Along the Minor Axis
Spherical aberration	0.136 (0.176)	0.229 (0.021)*	-0.022 (0.831)	-0.132 (0.190)	0.291 (0.003)*
Coma	0.282 (0.004)*	0.191 (0.056)	0.220 (0.027)*	-0.106 (0.291)	0.434 (< 0.001)*
Trefoil	0.100 (0.322)	0.162 (0.105)	-0.094 (0.348)	-0.020 (0.845)	0.085 (0.369)
Total HOAs	0.374 (< 0.001)*	0.302 (0.002)*	0.223 (0.025)*	-0.006 (0.952)	0.453 (< 0.001)*
LOAs	0.107 (0.286)	0.055 (0.583)	0.110 (0.237)	-0.207 (0.038)*	0.256 (0.010)*

HOAs, higher-order aberrations; LOAs, lower-order aberrations

*P value less than 0.05 showing statistical significance

this tolerance may be further enhanced along the major axis in oval-shaped EOZ. In our study, subgroup analysis confirmed that induced spherical aberration, coma, total HOAs, and LOAs were higher in group B (with greater decentration along the minor axis than the major axis), despite no significant difference in decentration. In other words, decentration from 0° to 45°, 135° to 225°, and 315° to 360° yields more favorable outcomes than decentration from 45° to 135° and 225° to 315° in the coordinate system along major and minor axes of EOZ. Previous studies have shown that decentration greater than 0.3 mm is associated with larger induced corneal aberrations in corneal refractive surgery [25, 26]. Our study is the first to find that not only the magnitude but also the direction of decentration can impact the postoperative outcomes. Given the strong positive correlation between the EOZ major axis angle and the preoperative cylinder axis, we suggest that the combined impacts of EOZ and decentration on visual quality should be considered after surgery. Additionally, surgeons may not need to risk corneal edema and suction loss to re-suction in cases of slight decentration along the axis of the cylinder. The VISUMAX 800 femtosecond laser represents the latest advancement in the SMILE platform, succeeding the VisuMax 500 used in our study. Its CentraLign assistant function provides real-time monitoring of treatment cone positioning relative to the corneal vertex, potentially reducing postoperative decentration in all directions and thereby improving visual quality. Varman et al. [27] have reported that the VISUMAX 800 demonstrates improved accuracy when correcting cylinder greater than 2 diopters compared to the VisuMax 500. However, further research is needed to directly compare the decentration and visual quality outcomes between these two laser systems, particularly for myopic astigmatism.

Correlation analysis revealed a significant association between increased spherical aberration and EOZ area, major axis, and minor axis across the WTR, ATR, and oblique astigmatism groups. Increases in coma and total HOAs were similarly correlated with EOZ parameters in both WTR and ATR groups. However, induced trefoil did not show a significant correlation with EOZ parameters in any group. These findings align with previous studies demonstrating a negative correlation between EOZ area and induced spherical aberration, coma, and total HOAs [18, 28]. Additionally, EOZ major and minor axes were correlated with induced spherical aberration [19]. Fu et al. [28]also reported a lack of significant association between trefoil and EOZ area, consistent with our results. Regarding the relationship between decentration and induced corneal aberrations, the magnitude of decentration is known to influence visual quality. In our study, total decentration correlated positively with coma and total HOAs, consistent with the findings of Lee et al. [25]. Lee et al. [25] demonstrated that induced changes in total HOAs, coma, vertical coma, and spherical aberration were significantly larger in eyes with a total decentered displacement > 0.335 mm compared to those with ≤ 0.335 mm. However, our correlation analysis also revealed that decentration displacement along the minor axis had a more comprehensive and pronounced impact on visual quality than other decentration components in myopic astigmatism. This finding supports our hypothesis that in myopic astigmatism with an oval-shaped EOZ, tolerance to decentration is reduced along the minor axis, underscoring the importance of minimizing decentration in this direction during SMILE procedures.

One limitation of this study is the lack of quantitative analysis regarding the relationship between EOZ and decentration tolerance, and its impact on visual quality warrants further investigation.

Conclusions

This study demonstrates favorable outcomes after SMILE surgery for different astigmatism types. Postoperative refractive errors, visual acuity, and induced corneal aberrations showed no significant differences between groups with WTR, ATR, and oblique astigmatism. The angle of the EOZ major axis, measured using Image J, was closely associated with the preoperative cylinder axis. The visual quality was more favorable in patients with greater decentration along the major axis than the minor axis in oval shaped EOZ. These findings provide new insights into the evaluating methods and effects of EOZ and decentration in the treatment of myopic astigmatism after SMILE surgery.

Acknowledgements
Not applicable.

Author contributions
Conception and design, XM and XZ; administrative support, XZ; data collection, XM, HD, ZY, XC and SH; data analysis and interpretation, XM; drafting of the manuscript, XM; critical revision of the manuscript, XM and XZ. All authors read and approved the final manuscript.

Funding
This work was supported by the National Natural Science Foundation of China (82271116), Hainan Province Clinical Medical Center, Science and Technology Planning Project of Hainan Province (ZDYF2022SHFZ326, LCYX202406), and Hainan Province Clinical Medical Center.

Data availability
The datasets used and analyzed during the current study are available from the corresponding author upon reasonable request.

Declarations

Ethics approval and consent to participate
This retrospective study was approved by the Ethics Committee of Hainan Eye Hospital at Zhongshan Ophthalmic Center (Sun Yat-sen University, China) (ethics acceptance number: 2023-041-01) and conducted in accordance with the Declaration of Helsinki. Informed consent was obtained from all patients prior to the study.

Consent for publication
This study was approved to be published by all authors.

Competing interests
The authors declare no competing interests.

Received: 25 November 2024 / Accepted: 25 February 2025
Published online: 11 March 2025

References

1. He S, Luo Y, Ye Y, et al. A comparative and prospective study of corneal biomechanics after SMILE and FS-LASIK performed on the contralateral eyes of high myopia patients. Ann Transl Med. 2022;10(13):730–730. https://doi.org/10.21037/atm-22-330.
2. Mohamed-Noriega K, Riau AK, Lwin NC, Chaurasia SS, Tan DT, Mehta JS. Early corneal nerve damage and recovery following small incision lenticule extraction (SMILE) and laser in situ keratomileusis (LASIK). Invest Ophthalmol Vis Sci. 2014;55(3):1823. https://doi.org/10.1167/iovs.13-13324.
3. Moshirfar M, McCaughey MV, Reinstein DZ, Shah R, Santiago-Caban L, Fenzl CR. Small-incision lenticule extraction. J Cataract Refract Surg. 2015;41(3):652–65. https://doi.org/10.1016/j.jcrs.2015.02.006.
4. Blum M, Lauer AS, Kunert KS, Sekundo W. 10-Year results of small incision lenticule extraction. J Refract Surg. 2019;35(10):618–23. https://doi.org/10.3928/1081597x-20190826-02.
5. Pedersen IB, Ivarsen A, Hjortdal J. Changes in astigmatism, densitometry, and aberrations after SMILE for low to high myopic astigmatism: A 12-Month prospective study. J Refract Surg. 2017;33(1):11–7. https://doi.org/10.3928/1081597x-20161006-04.
6. del Alió JL, Vargas V, Al-Shymali O, Alió JL. Small incision lenticule extraction (SMILE) in the correction of myopic astigmatism: outcomes and limitations - an update. Eye Vis. 2017;4(1). https://doi.org/10.1186/s40662-017-0091-9.
7. Reinstein DZ, Archer TJ, Vida RS, Carp GI, Reinstein JFR, McAlinden C. Objective and subjective quality of vision after SMILE for high myopia and astigmatism. J Refract Surg. 2022;38(7):404–13. https://doi.org/10.3928/1081597x-20220516-03.
8. Ivarsen A, Gyldenkerne A, Hjortdal J. Correction of astigmatism with small-incision lenticule extraction: impact of against-the-rule and with-the-rule astigmatism. J Cataract Refract Surg. 2018;44(9):1066–72. https://doi.org/10.1016/j.jcrs.2018.06.029.
9. Chow S, Chow LLW, Lee Chester, Chan TC. Astigmatism Correction Using SMILE. *Asia - Pacific Journal of Ophthalmology*. Published online 2019. https://doi.org/10.1097/01.apo.0000580140.74826.f5
10. Pérez-Izquierdo R, Rodríguez-Vallejo M, Matamoros A, et al. Influence of preoperative astigmatism type and magnitude on the effectiveness of SMILE correction. J Refract Surg. 2019;35(1):40–7. https://doi.org/10.3928/1081597x-20181127-01.
11. Nemeth G, Szalai E, Berta A, Modis L. Astigmatism prevalence and biometric analysis in normal population. Eur J Ophthalmol. 2013;23(6):779–83. https://doi.org/10.5301/ejo.5000294.
12. Wang Y, Mu J, Yang Y, et al. Prevalence and risk factors for astigmatism in 7 to 19-year-old students in Xinjiang, China: a cross-sectional study. BMC Ophthalmol. 2024;24(1). https://doi.org/10.1186/s12886-024-03382-0.
13. Ueno Y, Nomura R, Hiraoka T, Kinoshita K, Ohara M, Oshika T. Comparison of corneal irregular astigmatism by the type of corneal regular astigmatism. Sci Rep. 2021;11(1). https://doi.org/10.1038/s41598-021-95358-z.
14. Tabernero J, Klyce SD, Sarver EJ, Artal P. Functional optical zone of the cornea. Invest Ophthalmol Vis Sci. 2007;48(3):1053. https://doi.org/10.1167/iovs.06-0867.
15. Li M, Zhao J, Miao H, et al. Mild decentration measured by a Scheimpflug camera and its impact on visual quality following SMILE in the early learning curve. Invest Ophthalmol Vis Sci. 2014;55(6):3886. https://doi.org/10.1167/iovs.13-13714.
16. Wang X, Xia L. Evaluation of the effects of myopic astigmatism correction and anterior corneal curvature on functional optical zone after SMILE. J Refract Surg. 2023;39(2):135–41. https://doi.org/10.3928/1081597x-20221215-01.
17. Huang J, Zhou X, Qian Y. Decentration following femtosecond laser small incision lenticule extraction (SMILE) in eyes with high astigmatism and its impact on visual quality. BMC Ophthalmol. 2019;19(1). https://doi.org/10.1186/s12886-019-1153-7.
18. Liu S, Gu X, Zhang X, Zhao J, Zhou X. Achieved and functional optical zone in myopic eyes with high astigmatism after small incision lenticule extraction. J Refract Surg. 2022;38(4):243–9. https://doi.org/10.3928/1081597x-20220201-01.
19. Ding X, Fu D, Wang L, Zhou X, Yu Z. Functional optical zone and visual quality after Small-Incision lenticule extraction for high myopic astigmatism. Ophthalmol Ther. 2021;10(2):273–88. https://doi.org/10.1007/s40123-021-00330-9.
20. Taneri S, Arba-Mosquera S, Rost A, Hansson C, Dick HB. Results of thin-cap small-incision lenticule extraction. J Cataract Refract Surg. 2020;Publish Ahead of Print. https://doi.org/10.1097/j.jcrs.0000000000000470
21. Hou J, Wang Y, Lei Y, Zheng X. Comparison of effective optical zone after small-incision lenticule extraction and femtosecond laser–assisted laser in situ keratomileusis for myopia. J Cataract Refract Surg. 2018;44(10):1179–85. https://doi.org/10.1016/j.jcrs.2018.06.046.
22. Liang C, Yan H. Methods of corneal vertex centration and evaluation of effective optical zone in small incision lenticule extraction. Ophthalmic Res Published Online 2023:717–26. https://doi.org/10.1159/000529922
23. Huang Y, Ding X, Han T, Fu D, Yu Z, Zhou X. Effective optical zone following small incision lenticule extraction for myopia calculated with two novel methods. J Refract Surg. 2022;38(7):414–21. https://doi.org/10.3928/1081597x-20220608-02.

24. Huang Y, Zhan B, Han T, Zhou X. Effective optical zone following small incision lenticule extraction: a review. Graefes Arch Clin Exp Ophthalmol Published Online Oct. 2023;18. https://doi.org/10.1007/s00417-023-06263-2.
25. Lee H, Roberts CJ, Arba-Mosquera S, Kang DSY, Reinstein DZ, Kim T. im. Relationship Between Decentration and Induced Corneal Higher-Order Aberrations Following Small-Incision Lenticule Extraction Procedure. *Invest Ophthalmol Vis Sci*. 2018;59(6):2316. https://doi.org/10.1167/iovs.17-23451
26. Lee SB, Hwang BS, Lee J. Effects of decentration of photorefractive keratectomy on the induction of higher order wavefront aberrations. J Refract Surg. 2010;26(10):731–43. https://doi.org/10.3928/1081597x-20091209-01.
27. Varman A, Varman A, Balakumar D. Comparison of visual and refractive outcomes of keratorefractive lenticule extraction for compound myopic astigmatism between visumax and VISUMAX 800. OPTH. 2024;18:3557–66. https://doi.org/10.2147/opth.s492552.
28. Fu D, Wang L, Zhou X, Yu Z. Functional optical zone after Small-Incision lenticule extraction as stratified by attempted correction and optical zone. Cornea. 2018;37(9):1110–7. https://doi.org/10.1097/ico.0000000000001669.

Publisher's note